

Research Article

Synthesis, Characterization, and Drug Delivery from pH- and Thermoresponse Poly(N-Isopropylacrylamide)/Chitosan Core/Shell Nanocomposites Made by Semicontinuous Heterophase Polymerization

Abraham G. Alvarado,¹ Andres Ortega,² Lourdes A. Pérez-Carrillo,² Israel Ceja,³ Martin Arellano,² R. Guillermo López,⁴ and Jorge E. Puig²

¹Departamento de Ingeniería Mecánica Eléctrica, Universidad de Guadalajara, Boul. M. García-Barragán #1451, 44430 Guadalajara, JAL, Mexico

²Ingeniería Química, Universidad de Guadalajara, Boul. M. García-Barragán #1451, 44430 Guadalajara, JAL, Mexico

³Física, Universidad de Guadalajara, Boul. M. García-Barragán #1451, 44430 Guadalajara, JAL, Mexico

⁴Centro de Investigación en Química Aplicada, Av. Ing. E. Reyna #140, 25294 Saltillo, COAH, Mexico

Correspondence should be addressed to Jorge E. Puig; puigje@mail.udg.mx

Received 31 August 2016; Revised 16 December 2016; Accepted 19 December 2016; Published 24 January 2017

Academic Editor: Xuping Sun

Copyright © 2017 Abraham G. Alvarado et al. This is an open access article distributed under the Creative Commons Attribution License, which permits unrestricted use, distribution, and reproduction in any medium, provided the original work is properly cited.

Temperature- and pH-responsive core/shell nanoparticles were prepared by semicontinuous heterophase polymerization of N-isopropylacrylamide (NIPA) in the presence of chitosan micelles for drug delivery purposes. Micelles of chitosan, formed in an acetic acid aqueous solution at 70°C containing potassium persulfate, were fed with N-isopropylacrylamide (NIPA) at a controlled rate, to produce PNIPA/chitosan core/shell nanoparticles of about 350 nm. Then, the crosslinking agent, glutaraldehyde, was added to crosslink the nanoparticles. These nanocomposites were temperature- and pH-responsive, which make them suitable as controlled drug releasing agents. The nanoparticles exhibit thermoreversibility to heating-and-cooling cycles and show different responses depending on the releasing medium's pH. Drug delivery tests were performed, employing as a model drug, doxycycline hyclate.

1. Introduction

Environmentally sensitive nanoparticles (NPs) are receiving increasing scientific and industrial attention as drug-delivery systems because of their ability to release drugs to therapeutic targets at controlled and appropriate times and doses [1–5]. Their sizes of the order of a few tenths of nanometers allow them to go through capillary vessels avoiding being trapped by phagocytes, which permits larger duration in the blood stream.

Recently, biodegradable and biocompatible polymeric materials used for drug delivery have been developed, such as poly(lactic acid), poly(lactide-co-glycolide), polycaprolactone, polyanhydrides, poly(hydroxyalkanoates),

polypeptides, and polysaccharides [6–8]. Among them, polysaccharides are the most employed polymers to prepare NPs for drug delivery purposes [9, 10]. Chitosan (CS) is a polysaccharide that is pH-responsive due to its amino groups along the chain, which are able to get protonated at acid pHs [5].

Environmentally sensitive polymers have been investigated in biomedical applications such as drug delivery, sensors, diseases' targeting and diagnostics [11–13]. Among these polymers, poly(N-isopropylacrylamide) (PNIPA) is the most studied thermoresponse polymer because it has a lower critical solution temperature (LCST) of ca. 32–33°C [12]; below this temperature, PNIPA is completely soluble in water, but above it, PNIPA and water phase separate due to the

transition from a hydrophilic to a hydrophobic structure at this temperature [14].

Huang et al. reported in 2013 that chitosan was able to form micelles in an acetic acid solution, even though this polysaccharide is insoluble in pure water; these authors demonstrated the micelle formation and reported the critical micellar concentration by fluorescence emission spectroscopy [15]. In addition, Huang et al. showed, in the same article, that by adding NIPA in one shot and an initiator (potassium persulfate) at 70°C, the NIPA polymerized and because the reaction temperature was higher than the LCST of the PNIPA, it became hydrophobic and, as a consequence, migrated to the micellar core. To ensure that the PNIPA/CS micelles would not be disrupted in further applications, these authors added an aqueous solution of glutaric dialdehyde to crosslink the micelles; moreover, they demonstrated the capability for prolonged drug delivery of this core/shell PNIPA/CS micellar solution. Wang et al. synthesized core/shell nanomaterials through radical polymerization of CS and a mixture of NIPA and acrylamide (AM), which exhibited thermally sensitive features and that allowed to tune the volume phase transition temperature (T_{VPT}) up to collapsing temperatures of ca. 39°C, depending on the AM/NIPA molar ratio [16].

Popat et al. [17] reported a CS-coated mesoporous silica nanospheres that were pH-responsive and used ibuprofen as model drug; they demonstrated that, under basic conditions, the core/shell nanomaterial forms a gel structure that is insoluble and prevents the drug release, whereas below the CS isoelectric point (pH = 6.3), the drug is released due to the protonation of the CS amino groups. Chang et al. [18] produced poly[poly(ethylene glycol methyl ether methacrylate)-block-poly(methyl methacrylate)] block copolymer to encapsulate the model drug, Nile Red, and a chemotherapeutic drug, doxorubicin (DOX), and showed that the release of DOX from the micelles was sufficient to be cytotoxic to human colon carcinoma cells. Li et al. [19] developed a potential nanocarrier for topical administration of curcumin (CUR), a novel thiolated CS made by covalent binding between N-acetyl-L-cysteine (NAC) and CS, which was employed to modify the surface of the nanostructured lipid carrier CUR. Onnainty et al. [20] created sustained release systems of the drug, chlorhexidine (CLX), based on CS and montmorillonite. These hybrid carriers exhibited sustained release of CLX, which allowed maintaining the CLX antimicrobial properties.

In this study, we synthesized pH- and thermoresponsive NIPA/CS core/shell nanoparticles by semicontinuous heterophase polymerization (SHP). The aim was to synthesize thermo- and pH-sensitive nanoparticles with larger polymer content than those reported by Huang et al. [15] and evaluate their thermoreversibility and their potential application as drug carrier and delivery systems as a function of pH and temperature.

2. Experimental Section

CS, AM (99% pure), NMBA (99% pure), glutaraldehyde ((GA); 50 wt.% in water), and doxycycline (98% pure) were obtained from Sigma-Aldrich. NIPA was 99% pure from

Acros Organics; KPS (99% pure) was from Fermont; N₂ gas was from Infra de Occidente (México); and doubly distilled water was from Productos Selectopura (México).

The CS degree of deacetylation was determined potentiometrically with the following procedure: first 0.4 g of CS was dissolved in 89 g of a 0.1 M HCl solution by constant stirring during 24 h; next, this solution was titrated with 0.1393 M NaOH solution with a pH-meter. The volume of the NaOH solution added to the chitosan solution was plotted versus the measured pH to determine two inflection points that correspond to the excess HCl added volume and to the protonated CS volume, respectively. The difference between these two volumes corresponds to the amount of HCl consumed for the protonation of the amine groups of the chitosan, which allows the determination of the CS degree of deacetylation with the following formula:

$$\% \text{ DA} = 2.03 * \left(\frac{V_2 - V_1}{m + 0.0042 (V_2 - V_1)} \right). \quad (1)$$

Here m is the mass of the sample, V_1 and V_2 correspond to the volumes of NaOH solution where the inflection points were located, 2.03 is the coefficient resulting from the molar masses of the units of the CS monomer, and 0.0042 is the difference between the molar mass of the units of the monomers of quinine and CS. The calculated degree of deacetylation was 68%.

The viscosity-average molar mass (M_v) of the chitosan was determined in an Anton-Paar automatic Ubbelohde microviscosimeter. For these measurements, different amounts of CS were dissolved in 50 mL of a 0.2 M NaCl dissolved in 0.1 M of acetic acid aqueous solution with agitation for 24 h. Then samples were put in a constant-temperature water bath at 25°C and their shear viscosity was measured at the same temperature in the microviscosimeter. From the measured viscosity of the different samples, the intrinsic viscosity, $[\eta]$, was determined in the usual way. The viscosity-average molar mass was then calculated using the Mark-Houwkins equation given by

$$[\eta] = KM_v^a \quad (2)$$

with the Mark-Houwkins constants, $K = 1.8 \times 10^{-5}$ dL/g and $a = 0.93$, reported by Roberts and Domszy [21]. The obtained chitosan M_v was 1.2×10^6 g/mol.

For the synthesis of the PNIPA/CS core/shell nanoparticles, the following procedure was followed: 2 g of CS was mixed with 160 g of distilled water containing 0.7 g of acetic acid, which was added to a 500 mL three-month glass reactor; this mixture was maintained under constant stirring at room temperature for 12 h. Then the reactor was immersed in a water bath maintained at 70°C; next, 0.684 g of KPS dissolved in 10 g of water was added to the reactor, which was then bubbled with N₂ to remove the dissolved oxygen. Then, a solution of 20.62 g of NIPA and 0.839 g of NMBA, dissolved in 349 g of water, was fed at a controlled rate to the reactor during 233 min. After this time, the reaction was allowed to continue for 1 h to increase the concentration of produced PNIPA. The latex was cooled down to 40°C, followed by the

addition of GA solution to crosslink the CS shell. Samples were collected at given times to follow the particle size evolution with reaction time. The final latex, cooled to 25°C, was collected and put in a dialysis bag ($M_n = 11,200$ g/mol exclusion size), which was immersed in a large amount of distilled water to eliminate the residual monomers, initiator, and GA that had not reacted. This dialyzed sample was placed in a teflon box and put in a convection oven at 60°C to dry until constant weight was achieved. The sample was weighed and the final conversion was estimated with the following formula [15]:

$$X = \frac{W_{\text{DRY}} - W_{\text{CS}} - W_{\text{GA}}}{W_{\text{NIPA}} + W_{\text{NMBA}}}. \quad (3)$$

Here W_{DRY} , W_{CS} , W_{GA} , W_{NIPA} , and W_{NMBA} are the masses of the dry sample, chitosan, glutaraldehyde, NIPA, and NMBA, respectively.

For the drug loading in the PNIPA/CS nanoparticles, 0.2012 g of nanoparticles was dispersed in 80 g of water containing 0.021 g of doxycycline (mother solution), which was maintained with constant agitation at pH of 4.5 and 25°C at room temperature during 24 h. After incubation for 96 h, the dispersion solution was adjusted to pH of 9 and the drug-loaded nanoparticles were separated from the dispersion by centrifugation at 13,500 rpm for 5 min. Then the nanoparticles were dried by lyophilization and weighed. To estimate the amount of drug loaded into the nanoparticles, a calibration curve of absorbance versus doxycycline concentration was made by diluting the mother solution at pH = 9. Each of the diluted samples was put in a quartz cell, which was placed in a Thermoelectron UV-vis spectrophotometer (Genesis 10 UV), to measure the absorbance at the wavelength of 346 nm. The obtained calibration curve was a straight line with R -square standard deviation of 0.9995. To obtain the drug liberation profiles, 0.40 g of the drug-loaded nanoparticles was mixed with 5 mL of a 90 wt.% w/v NaCl aqueous solution and loaded in a dialysis bag of 1,000 Dalton molecular mass cut-off. The dialysis bag was then immersed in 195 mL of normal-saline solution. The drug release profile was determined at two different temperatures (25 and 37°C) and two pHs (2 and 7).

Particle size of the nanocomposites was measured with a Nanosize S-90 quasielastic light scattering (QLS) apparatus from Malvern Instrument at 25°C. For the measurements, 0.05 g of the latices obtained at different reaction times was dispersed in 10 g of water; from this dispersion, 3 mL was put in a glass cell for the measurements.

The morphology, shape, and size distribution of the nanocomposites was examined with a TESCAM Field-Emission Scanning Electron Microscope (FESEM). For these tests, 0.05 g of the nanoparticles was dispersed in 200 g of water; 0.02 g of this dispersion was deposited in a Cu plaque, frozen to -60°C for 24 h, and lyophilized at -40°C and 1×10^{-4} bar for 2 h. Then the sample was covered with a thin gold layer and analyzed in the FESEM.

The PNIPA/CS nanoparticles were also examined in a JEOL 1200 EXII transmission electron microscope (TEM). For this, one drop of latex, diluted 20 times, was deposited in

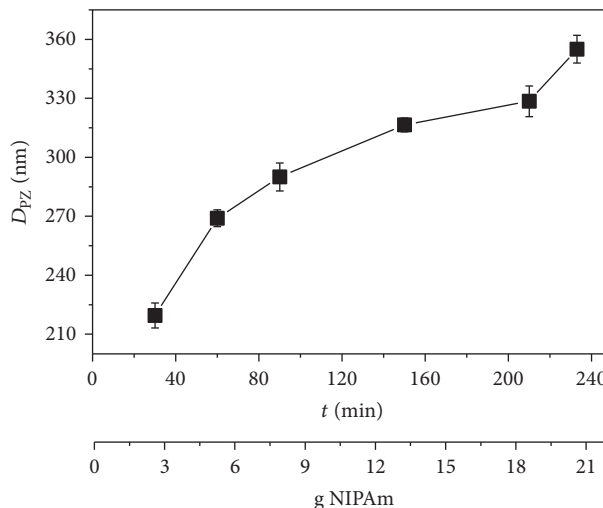


FIGURE 1: Evolution of particle size as a function of time and the dosed amount of NIPA.

a grid, which was dried overnight before observation in the TEM.

For the thermoreversibility and pH- and thermoresponse tests of the nanocomposites, 0.5 g of the dialyzed and dried nanoparticles were redispersed in 20 g of buffer solutions of pHs = 2, 4, and 7. Samples from these dispersions were placed in the glass cell for QLS measurements. The temperature range was from 20 to 50°C with increments of 5°C for the temperature-response tests; the equilibration time was of 15 min between temperature increments, to allow sample stabilization. Measurements were made three times for each sample. These temperature response tests were performed at three pHs (2, 4 and 7).

The thermoreversibility of the samples was examined using increasing-and-decreasing temperature cycles from 20 to 50°C as a measure of the stability. Measurements were made by QLS, allowing 15 min of equilibration at the end of each temperature increase or decrease. Again, these tests were performed at pHs of 2, 4, and 7.

3. Results

Figure 1 depicts the evolution of particle size in the presence of the CS micelles as a function of time and the dosed amount of NIPA. Initially, before the NIPA addition, the CS micelles have an average QLS size of ca. 200 nm, which is similar to that reported by Huang et al. [15], as expected. Clearly, particle size increased with increasing amount of NIPA added indicating that PNIPA was produced and that it was incorporated into the micellar core because, at the reaction temperature (70°C), this polymer is hydrophobic [14], and hence it enters the CS micelle hydrophobic core. Final particle size was ca. 360 nm but it increased to 380 ± 6 nm after the crosslinking of the CS micelles with GA.

Figure 2 shows a FESEM micrograph of the final nanocomposites. This micrograph shows polydispersed spheroidal particles with sizes of ca. 200 to 450 nm. This

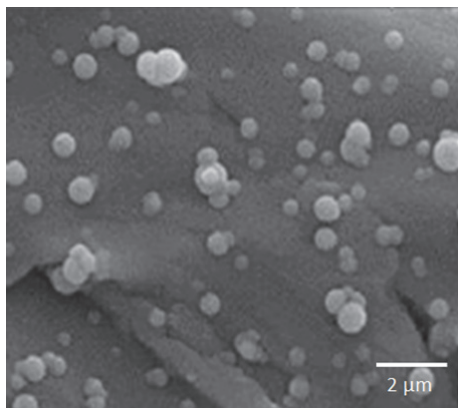


FIGURE 2: FESEM micrograph of the final nanocomposites.

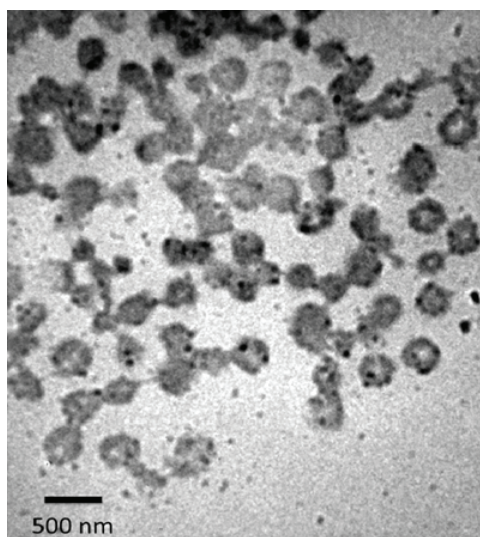


FIGURE 3: TEM micrograph of the obtained PNIPA/CS core/shell nanoparticles.

size polydispersity could be due to (i) aggregation during the polymerization of PNIPA; (ii) the treatment of the nanoparticles for FESEM examination which could have introduced agglomeration of the originally synthesized nanoparticles; and (iii) some PNIPA nanoparticles which did not penetrate the micelles, that is unlikely; moreover, PNIPA nanoparticles produced by semicontinuous heterophase polymerization (SHP) are much smaller, on the order of 30 nm as documented elsewhere [22].

Figure 3 depicts a TEM micrograph of the crosslinked PNIPA/CS nanoparticles. This micrograph reveals that the PNIPA/CS nanoparticles are spheroidal with average size of ca. 300 nm. Moreover, there is an obscure contour around each nanoparticle, which is due to the crosslinked CS micellar wall, surrounding the PNIPA nanoparticles that confirmed the formation of core/shell nanostructures. Moreover, no small particles (<50 nm), which might have formed due to the presence of PNIPA nanoparticles, are observed indicating that all the produced PNIPA entered into the CS micelles.

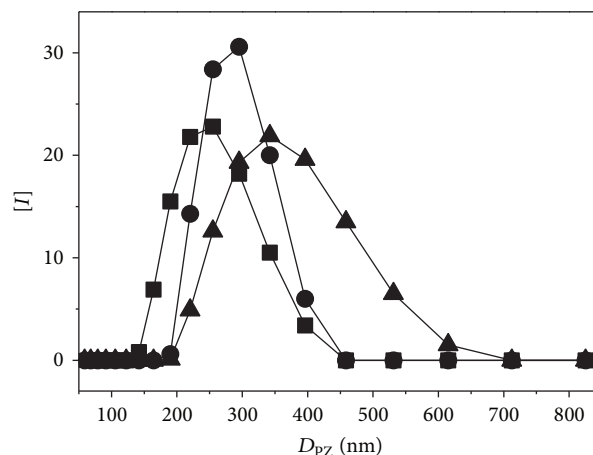


FIGURE 4: QLS-intensity size distribution of the reacting particles at three different reaction times, that is, 60 min (■), 160 min (●), and at the end of the reaction (▲).

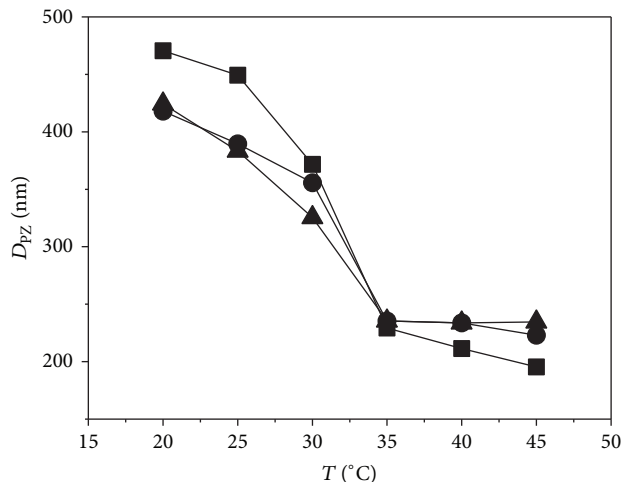


FIGURE 5: Particle size as a function of temperature measured at pHs of 2 (■), 4 (●), and 7 (▲).

Figure 4 shows QLS-intensity size distribution of the reacting particles at three different reaction times, that is, 60 min, 160 min, and at the end of the reaction. Clearly, size distributions shift to larger sizes as the reaction proceeds, in agreement with the average sizes shown in Figure 1. Moreover, particles are polydispersed, with sizes similar to those observed in the micrograph shown in Figure 1.

Figure 5 depicts plots of particle size as a function of temperature measured at three different pHs. The three reported curves exhibit an abrupt decrease in size with increasing the temperature from 20 to ca. 34°C and then the size reduction is substantially smaller. Notice that the inflection point (ca. 34°C) coincides with T_{VPT} of the crosslinked PNIPA at the three examined pHs, as expected since above T_{VPT} , PNIPA becomes hydrophobic and then it tends to expel the water trapped inside it. Notice that pH has a smaller but detectable effect in the swelling behavior of the nanocomposites, being larger at pH = 2 and smallest at pH = 7. As we will discuss later,

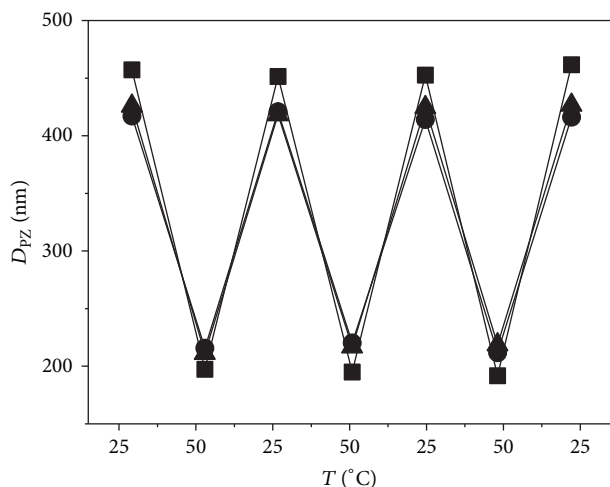


FIGURE 6: Thermoreversibility tests at the pHs of 2 (■), 4 (●), and 7 (▲).

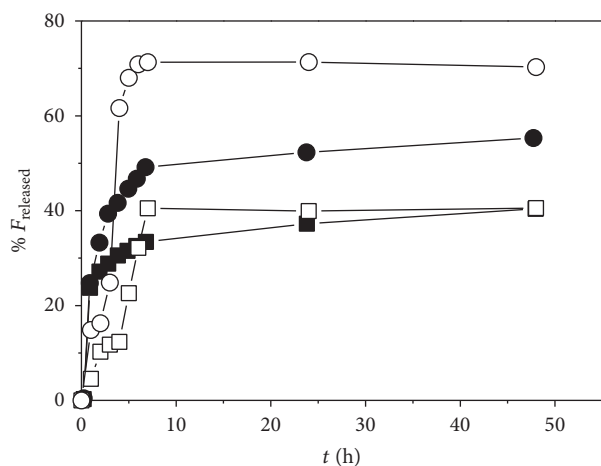


FIGURE 7: Drug liberation profiles measured at 25 (open symbols) and 37°C (closed symbols) at pHs of 2 (□, ■) and 7.4 (○, ●).

this is related to the interaction of CS and PNIPA groups with H^+ and OH^- groups at the different pHs and to the isoelectric point (pH = 6.3) of CS [23].

Figure 6 reports the thermoreversibility tests at the three pH used in this paper. The nanoparticles were subjected to heating-cooling-heating cycles as a function of pH to demonstrate whether or not the particles recovered their original sizes after the conclusion of the cycles. In all cases, samples recovered their sizes at all the three pHs examined, but now larger changes in size are detected at the more acid pH; these changes in sizes decreased as the pH was increased.

Figure 7 shows drug liberation profiles measured at 25 and 37°C at pHs of 2 and 7. The drug liberation profiles at both pHs increased rapidly during the first ca. 6 h, and then they rose more slowly but they kept raising even after 50 h of testing. Drug liberation is larger at pH = 2 compared to that at pH = 7.4 at both temperatures. However, drug release is larger at 25°C compared to those at 37°C, which seems contradictory with the fact that the PNIPA volume

phase transition temperature is ca. 34°C, and then it would be expected that the drug release would be larger at 37°C. Notice, however, that drug release is fast for both temperatures and pHs during the first 10 hrs, and then it diminishes substantially.

4. Discussion and Conclusions

Semicontinuous heterophase polymerization (SHP) is a variation of the semicontinuous microemulsion polymerization (SMP), which allows the synthesis of polymer nanoparticles and nanocomposites smaller than 50 nm with narrow size distributions, employing smaller amounts of surfactant and larger polymer-to-surfactant ratios compared to the SMP [24–28]. In this process and in contrast to the SMP, neat monomer is dosed at a controlled rate to an aqueous (or oleic) solution containing surfactant forming micelles, initiator, and a solvent-soluble initiator. An important feature of the SHP is that narrower particle size distributions with smaller molar masses, compared to SMP, are obtained. The SHP process has been proved successfully to synthesize a series of poly(alkyl methacrylates) that have anomalously higher glass transition temperatures, indicating a larger syndiotactic polymer content [24–28], semiconducting polypyrrole [29], mesoporous nanoparticles [30], and polymeric nanocomposites [31].

Here we report the synthesis of PNIPA/CS core/shell nanoparticles by SHP, determine their T_{VPT} , examine their thermoreversibility, observe their shape and size distribution by FESEM and TEM, and perform drug liberation tests with a model drug, doxycycline hyclate, as a function of temperature and pH. First, following the report of Huang et al. [15], CS micelles were produced in a dilute acetic acid solution, over which NIPA was dosed at a controlled rate and polymerized at 70°C to induce the formation of PNIPA and the subsequent entrapment in the CS micellar core since the reaction temperature (70°C) was higher than T_{VPT} of PNIPA, and, hence, the formed polymer molecules should migrate inside the micellar core. The growth of the initially formed CS micelles, which have a diameter of ca. 200 nm, increased with NIPA addition time as observed in Figure 1. Particles grew from ca. 200 nm to ca. 360 nm suggesting the incorporation of the formed PNIPA into the micellar core. QLS also show that the particles are polydispersed and grow with NIPA addition time (Figure 3), which indicates that most or all of the PNIPA formed was incorporated into the CS micellar core. TEM was used to determine the size and shape of the produced nanoparticles and it showed the presence of spheroidal nanoparticles (Figure 3) with sizes similar to those obtained by QLS. Moreover, TEM revealed the presence of a dark skin over the nanoparticles, which might be due to the thickness of the CS micelles around the PNIPA nanoparticles. QLS also showed that the polydispersed, single population, core/shell nanoparticles increased with reaction time (Figure 4).

To examine the response of temperature as a function of pH, the nanocomposites sizes were measured by QLS at different pHs. Results, shown in Figure 5, demonstrate that the PNIPA/CS core/shell nanoparticles shrink rapidly with

increasing temperature up to ca. 34°C, which correspond to the hydrophilic-hydrophobic transition of PNIPA (T_{VPT}), at which PNIPA collapses. The gradual size decrease of the nanoparticles is, hence, related to the expulsion of water by the PNIPA core as the temperature is increased. For temperature larger than 34°C, the size decrease of the nanoparticle is smaller since the remaining water in the particles continues to be expelled but in much smaller amounts. Notice that pH plays a role in the shrinking behavior of the nanocomposites, being larger at the more acid pH and then diminishing as the pH increases. Here the main role is played by the CS shell. This natural polymer has an ionization potential (IP) of 6.3 [23]. At pH values higher than this value, CS forms a gel-like structure that is insoluble and it reduces the water release, whereas at pH below its IP, water can be released because of the protonation of the amino groups of CS, producing a softer, more labile structure. An important feature of the PNIPA/CS nanoparticles is that they exhibit thermoreversibility after four consecutive heating-cooling-heating cycles (Figure 6) indicating that the nanoparticles structure is maintained and that they are thermoreversible; that is, they recover their original size and structure.

The PNIPA/CS core/shell nanoparticles made here by SHP were subjected to drug delivery tests to determine their potential as nanocarriers. As demonstrated in Figure 7, the PNIPA/CS nanoparticles were able to dose the model drug, doxycycline, in prolonged periods of time. As expected, due to the sensitivity of the CS shell to pH, drug release is larger at pH = 2 than at pH = 7, regardless of the test temperature. Drug release is fast at early releasing tests and then becomes slower after ca. 12 hrs for both temperatures and pHs. After 50 hrs, approximately the 55% of the drug had been released at pH = 2 and at 37°C and ca. 38% at pH = 7 at 37°C. Notice, however, that drug keeps being released even after 50 hrs, indicating that the PNIPA/CS core/shell nanoparticles exhibit long releasing activity. Moreover, temperature also has an important effect on the drug release profiles. As shown in Figure 7, drug release is larger at 25°C than at 37°C, which is contrary to our expectation inasmuch as PNIPA collapses at ca. 34°C. However, Huang et al. [15] proposed that, due to the collapsing of the PNIPA at temperatures larger than 34°C, the remaining drug molecules get trapped into the shrinking PNIPA core because some of the drug molecules had some interactions with PNIPA. These results suggest that some drug molecules get trapped in the core/shell nanoparticles inside the PNIPA nanocore even above the collapsing PNIPA temperature and that, below the T_{VPT} , the drug molecules are able to diffuse faster through the swollen PNIPA core and the CS shell.

To determine the diffusion mechanism of the liberated drug, several models were employed, mainly, those of order zero, first order, Higuchi, and Korsmeyer-Peppas [32]. Our results (not shown) indicate that the Korsmeyer-Peppas model is the one that fits better the drug release at earlier releasing times, which indicate that the diffusion is non-Fickian. This is to be expected inasmuch as the drug has to diffuse first from the PNIPA core to the CS shell before exiting the nanoparticles. Similar mechanisms has been proposed for the drug release from a polymeric matrix.

The comparison with Huang et al. [15] clearly demonstrates that larger concentrations of drug are released in similar times in our work, 47.1%, compared to 38% in Huang et al. after 7 hrs of dosing at 37°C, which is the temperature of interest for mammals drug release applications. Clearly, the differences in the drug releasing times could be explained in terms of the PNIPA molecular mass and internal structure, evidently affected by the polymerization method [33]. Huang et al. added the whole amount of NIPA over the CS micellar solutions, which were at 70°C; hence, one should expect a NIPA solution polymerization mechanism, which should produce low molecular weights and loose porous-structured particles [33]. However, the PNIPA produced by SHP has larger molecular weight and more compact crosslinked structure as shown elsewhere [22]. Hence, the release of trapped substance within these two different structures should be quite different, as is the case here.

In conclusion, we have reported here the synthesis by SHP of PNIPA/CS core/shell nanoparticles, which, when swollen with water, exhibit a fast size decrease at ca. 34°C due to the rapid expulsion of water, which is associated with T_{VPT} of PNIPA; at higher temperature size also diminishes but less rapidly with increasing temperature. The nanoparticles are also pH-responsive, specially at acid pHs, which is related to the transition from a soluble-to-insoluble gel structure of the CS. These nanoparticles were thermoreversible; that is, they recovered their size and shape after being submitted to heating-and-cooling cycles in the range of 25 to 50°C. QLS, FESEM, and TEM reveal that the nanoparticles are spheroidal and polydispersed. Liberation studies of a model drug were performed that demonstrate that the PNIPA/CS nanoparticles exhibit a long-release behavior, which makes them suitable as drug releasing carriers.

Competing Interests

The authors declare that they have no competing interests.

References

- [1] R. Langer and D. A. Tirrell, "Designing materials for biology and medicine," *Nature*, vol. 428, no. 6982, pp. 487–492, 2004.
- [2] F. Alexis, E. Pridgen, L. K. Molnar, and O. C. Farokhzad, "Factors affecting the clearance and biodistribution of polymeric nanoparticles," *Molecular Pharmaceutics*, vol. 5, no. 4, pp. 505–515, 2008.
- [3] Z. Liu, Y. Jiao, Y. Wang, C. Zhou, and Z. Zhang, "Polysaccharides-based nanoparticles as drug delivery systems," *Advanced Drug Delivery Reviews*, vol. 60, no. 15, pp. 1650–1662, 2008.
- [4] N. S. Rejinold, P. R. Sreerakha, K. P. Chennazhi, S. V. Nair, and R. Jayakumar, "Biocompatible, biodegradable and thermosensitive chitosan-g-poly (*N*-isopropylacrylamide) nanocarrier for curcumin drug delivery," *International Journal of Biological Macromolecules*, vol. 49, no. 2, pp. 161–172, 2011.
- [5] A. D. Sezer and E. Cevher, "Topical drug delivery using chitosan nano- and micro-particles," *Expert Opinion on Drug Delivery*, vol. 9, no. 9, pp. 1129–1146, 2012.

- [6] G. Berth, A. Voigt, H. Dautzenberg, E. Donath, and H. Möhwald, "Polyelectrolyte complexes and layer-by-layer capsules from chitosan/chitosan sulfate," *Biomacromolecules*, vol. 3, no. 3, pp. 579–590, 2002.
- [7] Y. Hu, X. Jiang, Y. Ding, H. Ge, Y. Yuan, and C. Yang, "Synthesis and characterization of chitosan-poly(acrylic acid) nanoparticles," *Biomaterials*, vol. 23, no. 15, pp. 3193–3201, 2002.
- [8] Y. Hu, Y. Ding, D. Ding et al., "Hollow chitosan/poly(acrylic acid) nanospheres as drug carriers," *Biomacromolecules*, vol. 8, no. 4, pp. 1069–1076, 2007.
- [9] C. Choi, J.-P. Nam, and J.-W. Nah, "Application of chitosan and chitosan derivatives as biomaterials," *Journal of Industrial and Engineering Chemistry*, vol. 33, pp. 1–10, 2016.
- [10] P. K. Dutta, Ed., *Chitin and Chitosan for Regenerative Medicine*, Springer Series of Polymer and Composite Materials, Springer, New York, NY, USA, 2016.
- [11] A. Yamada, Y. Hiruta, J. Wang, E. Ayano, and H. Kanazawa, "Design of environmentally responsive fluorescent polymer probes for cellular imaging," *Biomacromolecules*, vol. 16, no. 8, pp. 2356–2362, 2015.
- [12] Y. Isikver and D. Saraydin, "Environmentally sensitive hydrogels: N-isopropylacrylamide/acrylamide/mono-, di-, tricarboxylic acid crosslinked polymers," *Polymer Engineering and Science*, vol. 55, no. 4, pp. 843–851, 2014.
- [13] F. Sun, Y. Wang, Y. Wei, G. Cheng, and G. Ma, "Thermally triggered drug delivery from polymeric micelles of poly(N-isopropylacrylamide-co-acrylamide)-b-poly(n-butyl methacrylate) for tumor targeting," *Journal of Bioactive and Compatible Polymers*, vol. 29, no. 4, pp. 301–317, 2014.
- [14] H. G. Schild, "Poly(N-isopropylacrylamide): experiment, theory and application," *Progress in Polymer Science*, vol. 17, no. 2, pp. 163–249, 1992.
- [15] C.-H. Huang, C.-F. Wang, T.-M. Don, and W.-Y. Chiu, "Preparation of pH- and thermo-sensitive chitosan-PNIPAAm core-shell nanoparticles and evaluation as drug carriers," *Cellulose*, vol. 20, no. 4, pp. 1791–1805, 2013.
- [16] Y. Wang, H. Xu, L. Ge, and J. Zhu, "Development of a thermally responsive nanogel based on chitosan-poly(N-isopropyl-co-acrylamide) for paclitaxel delivery," *Pharmaceutics, Drug Delivery and Pharmaceutical Technology*, vol. 103, pp. 2012–2021, 2014.
- [17] A. Popat, J. Liu, G. Q. Lu, and S. Z. Qiao, "A pH-responsive drug delivery system based on chitosan coated mesoporous silica nanoparticles," *Journal of Materials Chemistry*, vol. 22, no. 22, pp. 11173–11178, 2012.
- [18] T. Chang, P. Gosain, M. H. Stenzel, and M. S. Lord, "Drug loading of poly[(polyethylene glycol methyl ether methacrylate)-block-poly(methyl methacrylate)] (PEGMEMA)-based micelles and mechanisms of uptake in colon carcinoma cells," *Colloid and Surfaces B—Biointerfaces*, vol. 144, pp. 257–264, 2016.
- [19] J. Li, D. Liu, G. Tan, Z. Zhao, X. Yang, and W. Pan, "A comparative study on the efficiency of chitosan-N-acetylcysteine, chitosan oligosaccharides or carboxymethyl chitosan surface modified nanostructured lipid carrier for ophthalmic delivery of curcumin," *Carbohydrate Polymers*, vol. 146, pp. 435–444, 2016.
- [20] R. Onnainty, B. Onida, P. Páez, M. Longhi, A. Barresi, and G. Granero, "Targeted chitosan-based bionanocomposites for controlled oral mucosal delivery of chlorhexidine," *International Journal of Pharmaceutics*, vol. 509, no. 1–2, pp. 408–418, 2016.
- [21] G. A. F. Roberts and J. G. Domszy, "Determination of the viscometric constants for chitosan," *International Journal of Biological Macromolecules*, vol. 4, no. 6, pp. 374–377, 1982.
- [22] J. Aguilar, F. Moscoso, O. Rios et al., "Swelling behavior of poly(N-isopropylacrylamide) nanogels with narrow size distribution made by semi-continuous inverse heterophase polymerization," *Journal of Macromolecular Science, Part A: Pure and Applied Chemistry*, vol. 51, no. 5, pp. 412–419, 2014.
- [23] T. López-León, E. L. S. Carvalho, B. Seijo, J. L. Ortega-Vinuesa, and D. Bastos-González, "Physicochemical characterization of chitosan nanoparticles: electrokinetic and stability behavior," *Journal of Colloid and Interface Science*, vol. 283, no. 2, pp. 344–351, 2005.
- [24] M. G. Pérez-García, M. Rabelero, S. M. Nuño-Donlucas et al., "Semicontinuous heterophase polymerization of butyl methacrylate: effect of monomer feeding rate," *Journal of Macromolecular Science Part A. Pure and Applied Chemistry*, vol. 49, no. 7, pp. 539–546, 2012.
- [25] M. G. Pérez-García, E. V. Torres, I. Ceja et al., "Semicontinuous heterophase copolymerization of styrene and acrylonitrile," *Journal of Polymer Science A: Polymer Chemistry*, vol. 50, no. 16, pp. 3332–3339, 2012.
- [26] M. G. Pérez-García, A. G. Alvarado, M. Rabelero et al., "Semicontinuous heterophase polymerization of methyl and hexyl methacrylates to produce latexes with high nanoparticles content," *Journal of Macromolecular Science A: Pure and Applied Chemistry*, vol. 51, no. 2, pp. 144–155, 2014.
- [27] M. G. Pérez García, A. G. Alvarado, L. A. Pérez-Carrillo et al., "On the modeling of the semicontinuous heterophase polymerization of alkyl methacrylates with different water solubilities," *Macromolecular Reaction Engineering*, vol. 9, no. 2, pp. 114–124, 2015.
- [28] H. Saade, C. Barrera, G. Guerrero, E. Mendizábal, J. E. Puig, and R. G. López, "Preparation and loaded with rifampicin of sub-50 nm poly(ethyl cyanoacrylate)," *Journal of Nanomaterials*, vol. 2016, Article ID 384973, 11 pages, 2016.
- [29] J. C. González-Iñiguez, V. M. Ovando-Medina, C. F. Jasso-Gastinel, D. A. González, J. E. Puig, and E. Mendizábal, "Synthesis of polypyrrole nanoparticles by batch and semicontinuous heterophase polymerizations," *Colloid and Polymer Science*, vol. 292, no. 6, pp. 1269–1275, 2014.
- [30] O. Esquivel, M. E. Treviño, H. Saade, J. E. Puig, E. Mendizábal, and R. G. López, "Mesoporous polystyrene nanoparticles synthesized by semicontinuous heterophase polymerization," *Polymer Bulletin*, vol. 67, no. 2, pp. 217–226, 2011.
- [31] J. E. Puig and M. Rabelero, "Semicontinuous microemulsion polymerization," *Current Opinion in Colloid and Interface Science*, vol. 25, pp. 83–88, 2016.
- [32] G. Singhvi and M. Sing, "Review: in-vitro drug release characterization models," *International Journal of Pharmaceutical Studies and Research*, vol. 2, no. 1, pp. 77–84, 2011.
- [33] G. Odian, *Principles of Polymerization*, Wiley Interscience, New York, NY, USA, 2004.



Hindawi

Submit your manuscripts at
<https://www.hindawi.com>

